

Deconfinement to Quark Matter in Magnetars

Veronica Dexheimer

UFSC, Florianopolis, BR
Gettysburg College, Gettysburg, USA

E-mail: vantoche@gettysburg.edu

Rodrigo Nereiros

Instituto de Fisica, UFF, Niteroi, BR

Stefan Schramm

FIAS - Johann Wolfgang Goethe University, Frankfurt, DE

Abstract. We model magnetars as hybrid stars, which have a core of quark matter surrounded by hadronic matter. For this purpose, we use an extended version of the SU(3) non-linear realization of the sigma model in which the degrees of freedom change naturally from hadrons to quarks as the temperature/density increases. The presence of a variable magnetic field allows us to study in detail the influence of Landau quantization and the anomalous magnetic moment on the particle population of the star, more precisely on particles with different spin projections. This allows us to calculate the polarization of the system throughout different phases of the star, hadronic, quark and also a mixed phase.

1. Introduction and Model Description

Magnetars are compact stars that have extremely high magnetic fields. The highest magnetic field observed on the surface of a star is on the order of 10^{15} G. The highest possible magnetic field in the center of stars, on the other hand, can only be estimated through models, even when applying the virial theorem. Some results indicate limiting magnetic fields ranging between $B = 10^{18} - 10^{20}$ G [1–8]. Here we assume that magnetars are not necessarily composed of hadronic matter and describe them using a model that contains both hadronic and quark degrees of freedom.

Within this approach, the hadrons (whole baryon octet) are replaced by quarks (up, down, strange) at high densities and/or temperatures. This happens as the effective masses of the hadrons increase and the effective masses of the quarks decrease within these limits. The aforementioned model (see Ref. [9] for details) is an extended version of the SU(3) non-linear realization of the sigma model within the mean-field approximation. Changes in the order parameters of the model σ and Φ signal chiral symmetry restoration and quark deconfinement, respectively. The potential for Φ is an extension of the Polyakov loop potential [10] modified to also depend on baryon chemical potential. In this way our model is able to describe the entire QCD phase diagram, even at zero temperature. Fig. 1 shows that the model is in good agreement with lattice QCD constraints [11] and that it reproduces the liquid-gas phase

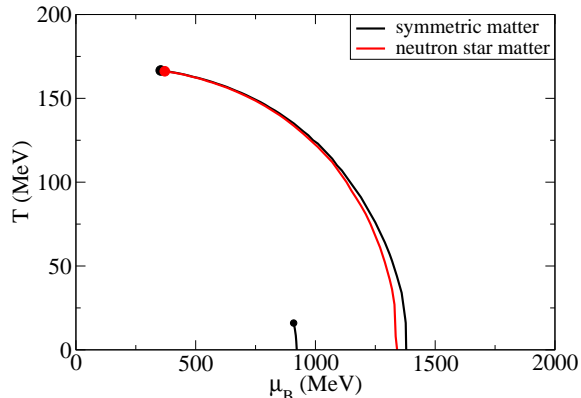


Figure 1. (Color online) QCD Phase Diagram - Temperature as a function of baryon chemical potential showing first-order phase transitions. The dots represent critical points.

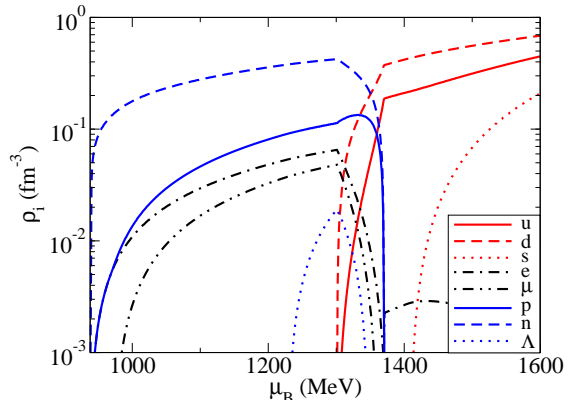


Figure 2. (Color online) Particle densities as a function of baryon chemical potential assuming global charge neutrality and chemical equilibrium at $T=0$. Quark densities are divided by 3.

transition for symmetric matter. In this figure we also show results for neutron star matter, which is charge neutral and in chemical equilibrium. The phase transitions at low temperatures and high densities are of first order, whereas at high temperatures and low densities the model exhibits smooth crossovers.

The SU(3) non-linear realization of the sigma model and its extension (that also contains quarks) have been successful in reproducing nuclear matter properties [12], heavy ion collision data [13], compact star and proto-neutron star properties [14–16]. As compact stars have temperatures of the order of 1 MeV, we can safely set their temperature to zero. As already mentioned, for star calculations we have to take into account charge neutrality and chemical equilibrium. Here we assume that the surface tension between the hadronic and quark phases is small [17] and allow charge neutrality to be global (only the combination of both phases sum up to zero charge). As a consequence, a mixed phase appears in the star. This can be seen in Fig. 2, which also shows that hyperons are almost completely suppressed by the appearance of the quarks.

We include in the model a magnetic field in the z -direction that has varying magnitude. This is a more realistic approach than considering a constant magnetic field throughout the star and can prevent the creation of hydrodynamical instabilities due to pressure anisotropy [18–22]. This happens because, in our approach, the magnetic field only becomes extremely high in the center of the star, where the matter pressure is also high (see Ref. [23] for more details). More precisely, we assume an effective magnetic field B^* that increases with chemical potential, running from a surface value $B_{surf} = 69.25 \text{ MeV}^2 = 10^{15} \text{ G}$ (when $\mu_B = 938 \text{ MeV}$) to different central values B_c at large values of baryon chemical potential following [16]

$$B^*(\mu_B) = B_{surf} + B_c \left[1 - e^{b \frac{(\mu_B - 938)^a}{938}} \right], \quad (1)$$

with $a = 2.5$, $b = -4.08 \times 10^{-4}$ and μ_B given in MeV. As can be seen in Fig. 3, the values of the effective magnetic field only approach B_c at very high baryon chemical potentials and, in practice, only about 70% of B_c can be reached inside stars. The use of an explicit dependence of B on the baryon chemical potential instead of on density was chosen to prevent discontinuities in the magnetic field at the phase transition, where the baryon density is discontinuous. The constants a and b and the form of the B^* expression were chosen to reproduce (in the absence of quarks) the effective magnetic field curve as a function of density from Refs. [5, 24, 25].

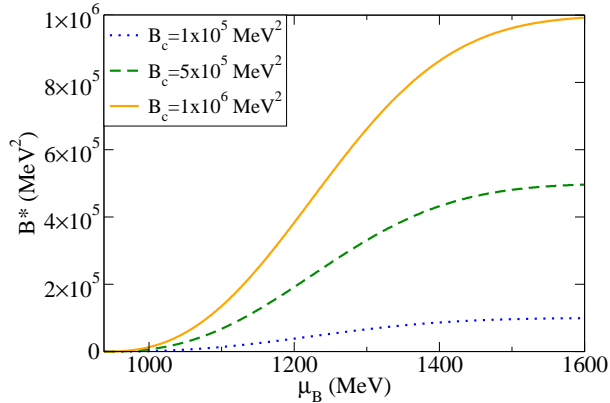


Figure 3. (Color online) Effective magnetic field as a function of baryon chemical potential shown for different central magnetic fields. Recall that using Gaussian natural units $1 \text{ MeV}^2 = 1.44 \times 10^{13} \text{ G}$.

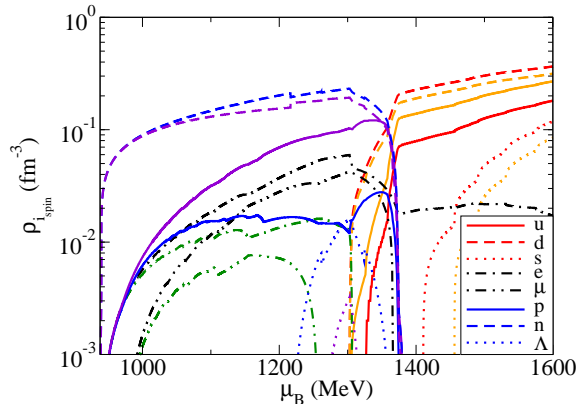


Figure 4. (Color online) Particle densities as a function of baryon chemical potential for $B_c = 5 \times 10^5 \text{ MeV}^2 = 7.22 \times 10^{18} \text{ G}$ including AMM. Black, blue and red stand for negative, while green, purple and orange stand for positive spin projections. Quark densities are divided by 3.

2. Results and Conclusions

The magnetic field in the z-direction forces the eigenstates in the x and y directions of charged particles to be quantized into Landau levels. The energy levels of all baryons are further split due to the alignment/anti-alignment of their spins with the magnetic field (anomalous magnetic moment effect, AMM). But even when the AMM is not taken into account, like in the quark phase in our model, only one of the spin projections contributes to the zeroth Landau level, creating a spin projection asymmetry in the system. In this work, we focus on the analysis of magnetic field effects on the chemical composition of the neutron star, the total spin polarization and the magnetization of the system. Studies of magnetic field effects on compact star observables can be found in Refs. [16, 26–28].

The particle population is shown in Fig. 4 when a central magnetic field $B_c = 5 \times 10^5 \text{ MeV}^2 = 7.22 \times 10^{18} \text{ G}$ with AMM is considered. The “wiggles” in the charged particle densities mark the μ_B values, for which their Fermi energies cross the discrete threshold of a Landau level. The charged particle population is enhanced due to B , as their chemical potentials increase. Although the AMM is known to make the EOS stiffer, it does not have a very significant effect in the particle population. This fact can be easily understood in terms of polarization, when, instead of looking at the total particle density (sum of spin up and down particle densities) for each species, we look at the spin up/spin down particle densities separately. In this case some of these particles are enhanced while others are suppressed (see Ref. [29] for details).

The total polarization of the system is defined as

$$\frac{\sum_i Q_{Bi}(\rho_{+i} - \rho_{-i})}{\sum_i Q_{Bi}(\rho_{+i} + \rho_{-i})}, \quad (2)$$

where Q_{Bi} stands for the baryon number of each species (3 for baryons, 1 for quarks and 0 for leptons). We can see in Fig. 5 that the total polarization of the system (taking into account hadrons and quarks) is larger for larger magnetic fields and increases with chemical potential until the quarks appear. After this point the polarization decreases. This happens because the AMM for the quarks is not included in our calculations, as it is not fully understood for

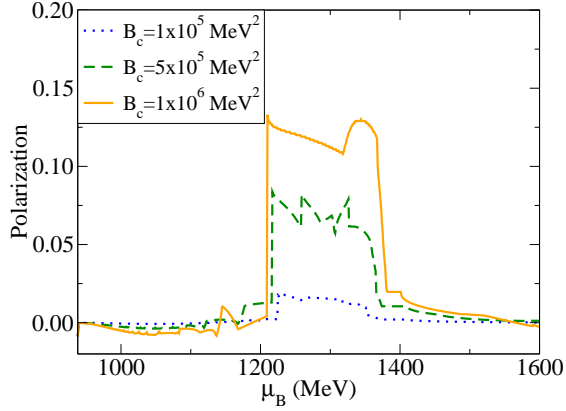


Figure 5. (Color online) Total spin polarization as a function of baryon chemical potential for different central magnetic fields (with $1 \text{ MeV}^2 = 1.44 \times 10^{13} \text{ G}$) including AMM.

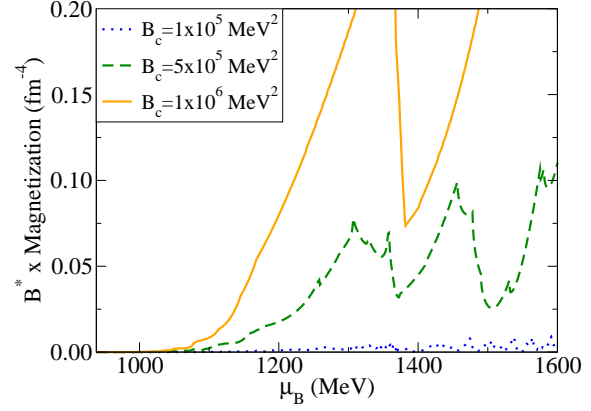


Figure 6. (Color online) Effective magnetic field times magnetization as a function of baryon chemical potential for different central magnetic fields (with $1 \text{ MeV}^2 = 1.44 \times 10^{13} \text{ G}$) including AMM.

these particles. In this case, the spin asymmetry comes exclusively from the spin asymmetric contribution to the zeroth Landau level. For an example of a complete study of the polarization without the AMM see Ref. [30]. The “wiggles” in Fig. 5 mark again when the Fermi energies of the charged particles cross the discrete threshold of a Landau level.

Finally, we turn our attention to the calculation of the magnetization of the system. It is important to notice that in the case with the AMM, not only the magnetization of the charged particles has to be included, but also the magnetization of the uncharged particles. For details on the calculation of the magnetization including the AMM see Ref. [31]. Fig. 6 shows that the magnetization is larger for larger magnetic fields and it increases with baryon chemical potential. As in Figs. 4 and 5, the “wiggles” mark when the Fermi energies of the charged particles cross the discrete threshold of a Landau level. The magnetization of the system is a very important quantity as it relates with the pressure anisotropy of the system [18–22].

We have shown in this work some possible effects of strong magnetic fields in hybrid stars. The presence of different hadronic and quark degrees of freedom makes this quark-hadron sigma model an ideal tool for such an analysis in the different possible phases of the star. More specifically, we analyzed the effects of strong chemical potential dependent magnetic fields on particles with different spin projections, their total polarization and magnetization.

Acknowledgments

V. D. acknowledges support from CNPq (National Counsel of Technological and Scientific Development - Brazil).

References

- [1] Bocquet M, Bonazzola S, Gourgoulhon E and Novak J 1995 *Astron.Astrophys.* **301** 757 (*Preprint gr-qc/9503044*)
- [2] Cardall C Y, Prakash M and Lattimer J M 2001 *Astrophys.J.* **554** 322–339 (*Preprint astro-ph/0011148*)
- [3] Lai D and Shapiro S L 1991 *Astrophys. J.* **383** 745–751
- [4] Chakrabarty S, Bandyopadhyay D and Pal S 1997 *Phys.Rev.Lett.* **78** 2898–2901 (*Preprint astro-ph/9703034*)
- [5] Bandyopadhyay D, Chakrabarty S and Pal S 1997 *Phys. Rev. Lett.* **79** 2176–2179 (*Preprint astro-ph/9703066*)
- [6] Broderick A E, Prakash M and Lattimer J M 2002 *Phys. Lett.* **B531** 167–174 (*Preprint astro-ph/0111516*)
- [7] Ferrer E J, de la Incera V, Keith J P, Portillo I and Springsteen P P 2010 *Phys. Rev.* **C82** 065802 (*Preprint 1009.3521*)
- [8] Malheiro M, Ray S, Mosquera Cuesta H J and Dey J 2007 *Int.J.Mod.Phys.* **D16** 489–499 (*Preprint astro-ph/0411675*)
- [9] Dexheimer V A and Schramm S 2010 *Phys. Rev.* **C81** 045201 (*Preprint 0901.1748*)
- [10] Roessner S, Ratti C and Weise W 2007 *Phys.Rev.* **D75** 034007 (*Preprint hep-ph/0609281*)
- [11] Fodor Z and Katz S 2004 *JHEP* **0404** 050 (*Preprint hep-lat/0402006*)
- [12] Papazoglou P *et al.* 1999 *Phys. Rev.* **C59** 411–427 (*Preprint nucl-th/9806087*)
- [13] Steinheimer J, Dexheimer V, Petersen H, Bleicher M, Schramm S *et al.* 2010 *Phys.Rev.* **C81** 044913 (*Preprint 0905.3099*)
- [14] Dexheimer V and Schramm S 2008 *Astrophys. J.* **683** 943–948 (*Preprint 0802.1999*)
- [15] Negreiros R, Dexheimer V and Schramm S 2010 *Phys.Rev.* **C82** 035803 (*Preprint 1006.0380*)
- [16] Dexheimer V, Negreiros R and Schramm S 2011 (*Preprint 1108.4479*)
- [17] Pinto M B, Koch V and Randrup J 2012 *Phys.Rev.* **C86** 025203 (*Preprint 1207.5186*)
- [18] Chaichian M, Masood S, Montonen C, Perez Martinez A and Perez Rojas H 2000 *Phys.Rev.Lett.* **84** 5261–5264 (*Preprint hep-ph/9911218*)
- [19] Perez Martinez A, Perez Rojas H, Mosquera Cuesta H J, Boligan M and Orsaria M G 2005 *Int. J. Mod. Phys.* **D14** 1959 (*Preprint astro-ph/0506256*)
- [20] Perez Martinez A, Perez Rojas H and Mosquera Cuesta H 2008 *Int. J. Mod. Phys.* **D17** 2107–2123 (*Preprint 0711.0975*)
- [21] Huang X G, Huang M, Rischke D H and Sedrakian A 2010 *Phys.Rev.* **D81** 045015 (*Preprint 0910.3633*)
- [22] Paulucci L, Ferrer E J, de la Incera V and Horvath J E 2011 *Phys. Rev.* **D83** 043009 (*Preprint 1010.3041*)
- [23] Dexheimer V, Menezes D and Strickland M 2012 (*Preprint 1210.4526*)
- [24] Mao G J, Iwamoto A and Li Z X 2003 *Chin. J. Astron. Astrophys.* **3** 359–374 (*Preprint astro-ph/0109221*)
- [25] Rabhi A, Pais H, Panda P K and Providencia C 2009 *J. Phys.* **G36** 115204 (*Preprint 0909.1114*)
- [26] Menezes D, Benghi Pinto M, Avancini S and Providencia C 2009 *Phys.Rev.* **C80** 065805 (*Preprint 0907.2607*)
- [27] Menezes D, Benghi Pinto M, Avancini S, Perez Martinez A and Providencia C 2009 *Phys.Rev.* **C79** 035807 (*Preprint 0811.3361*)
- [28] Avancini S S, Menezes D P and Providencia C 2011 *Phys. Rev. C* **83** 065805
- [29] Dexheimer V, Negreiros R, Schramm S and Hempel M 2012 (*Preprint 1208.1320*)
- [30] Isayev A and Yang J 2012 (*Preprint 1210.3322*)
- [31] Strickland M, Dexheimer V and Menezes D P 2012 (*Preprint 1209.3276*)